# Primary and secondary organic aerosols in 2016 summer of Beijing

Rongzhi Tang[1], Zepeng Wu[1], Xiao Li[1], Yujue Wang[1], Dongjie Shang[1], Yao Xiao[1], Mengren Li[1], Limin Zeng[1], Zhijun Wu[1], Mattias Hallquist[2], Min Hu[1], Song Guo[1,*]

[1]*State Key Joint Laboratory of Environmental Simulation and Pollution Control, College of Environmental Sciences and Engineering, Peking University, Beijing, 100871, PR China*

[2] *Atmospheric Science, Department of Chemistry and Molecular Biology, University of Gothenburg, Sweden*

[*] Correspondence to: Song Guo, songguo@pku.edu.cn

# Abstract

To improve the air quality, Beijing government has employed several air pollution control measures since 2008 Olympics. In order to investigate the organic aerosol sources after the implementation of these measures, ambient fine particulate matters were collected at a regional site Changping (CP) and an urban site Peking University Atmosphere Environment MonitoRing Station (PKUERS) during the "Photochemical Smog in China" field Campaign in summer of 2016. A chemical mass balance (CMB) modeling and the tracer yield method were used to apportion the primary and secondary organic sources. Our results showed that the particle concentration decreased significantly during the last a few years. The apportioned primary and secondary sources explained $62.8 \pm 18.3\%$ and $80.9 \pm 27.2\%$ of the measured OC at CP and PKUERS, respectively. Vehicular emissions served as the dominant sources. Except gasoline engine emission, the contributions of all the other primary sources decreased. Besides, the anthropogenic SOC, i.e. toluene SOC, also decreased, implying that deducting primary emission can reduce anthropogenic SOA. Different from the SOA from other regions in the world, where biogenic SOA was dominant, anthropogenic SOA was the major contributor to SOA, implying that deducting anthropogenic VOCs emissions is an efficient way to reduce SOA in Beijing. Back trajectory cluster analysis results showed that high mass concentrations of OC were observed when the air mass was from south. However, the contributions of different primary organic sources were similar, suggesting the regional particle pollution. The ozone concentration and temperature correlated well with the SOA concentration. Different correlations between day and night samples suggested the different SOA formation pathways. Significant enhancement of SOA with increasing particle water content and acidity were observed in our study, suggesting the aqueous phase acid-catalyzed reactions may be the important SOA formation mechanism in summer of Beijing.

## 1. Introduction

Beijing is the capital and a major metropolis of China. With the rapid economic growth and urbanization, Beijing is experiencing serious air pollution problems, and became one of the hotspots of $PM_{2.5}$ (particular matters with size smaller than 2.5μm) pollution in the world (Guo et al., 2014a; Xiang et al., 2017; Tian et al., 2016). Due to the frequent haze events in Beijing, Beijing government has taken a series of control measures in recent years, especially after 2008 Olympics, which may greatly influence the primary and secondary particle sources. Therefore, elucidating the current contributions of primary particle sources as well as secondary particle sources is of vital importance. It is also important to compare with the previous results to evaluate the effectiveness of the control measures and shed light on the influence of the primary source emission control on the secondary aerosol formation.

Several studies regarding to the source apportionment of fine particles in Beijing have been conducted using multifarious methods during the last few years (Yu et al., 2013; Gao et al., 2014; Zheng et al., 2016b; Tan et al., 2014; Wang et al., 2009; Guo et al., 2013). Receptor model is a commonly used method to apportion the particle sources (Zhang et al., 2017; Zhou et al., 2017; Zhang et al., 2013; Song et al., 2006; Zheng et al., 2005). Elemental tracers were previously used to apportion particulate matter sources (Yu et al., 2013; Gao et al., 2014; Zheng et al., 2016b). However, elemental tracer-based method was unable to distinguish sources that mostly emit organic compounds instead of specific elements such as diesel/gasoline engines. Among all the apportionment methods, chemical mass balance (CMB) model was one of the most commonly used methods to apportion the primary organic sources of fine particulate matter (Zhang et al., 2017; Hu et al., 2015; Schauer et al., 1996). Organic tracers have been successfully used in several studies which aimed to quantify the main sources of Beijing (Liu et al., 2016; Guo et al., 2013; Wang et al., 2009). Wang et al. assessed the source contributions of carbonaceous aerosol during 2005 to 2007

(Wang et al., 2009). Guo et al. (Guo et al., 2013) and Liu et al. (Liu et al., 2016) apportioned the organic aerosol sources using CMB model in summer of 2008 and a severe haze event in winter of 2013. Both studies found that vehicle emission and coal combustion were the dominant primary sources of fine organic particles. Tracer-yield method has been considered as a useful tool to semi-quantify SOA derived from specific VOCs precursors (Guo et al., 2012; Zhu et al., 2017; Zhu et al., 2016; Tao et al., 2017; Hu et al., 2008). However, only a few studies have estimated secondary organic aerosol in Beijing. Yang et al. (Yang et al., 2016) estimated the biogenic SOC to OC during CAREBEIJING-2007 field campaign, and found that the biogenic SOC accounted for 3.1% of the measured OC. Guo et al. (Guo et al., 2012) illustrated the SOA contributions in 2008, and found that secondary organic carbon could contribute a great portion (32.5 ±15.9%) to measured organic carbon at the urban site. Ding et al. (Ding et al., 2014) used the tracer-yield method to investigate the SOA loading on a national scale and found that SOA, especially anthropogenic SOA played great role in major city clusters of China.

In this study, we quantified 144 kinds of particulate organic species, including primary and secondary organic tracers, at a regional site and an urban site of Beijing. A CMB modeling and the tracer yield method were used to apportion the primary and secondary sources of the organic aerosols in the 2016 summer of Beijing. The results were compared with the previous studies to evaluate the effectiveness of control measures on primary as well as secondary organic aerosols. Moreover, source apportionment results from different air mass origins according to the back trajectory clustering analysis were shown to investigate the influences of air mass from different directions on the fine organic particle sources. Influencing factors of SOA formation, i.e. temperature, oxidant concentration, aerosol water content, as well as particle acidity were also discussed in this study to improve our understanding of SOA formation under polluted environment.

## 2. Experimental

### 2.1 Sampling and Chemical Analysis

The measurements were conducted simultaneously at an urban site Peking University Atmosphere Environment MonitoRing Station (PKUERS, 39°59′21″ N, 116°18′25″ E) and a regional site Changping (CP, 40°8′24″N, 116°6′36″ E) 40km north of PKUERS site during "Photochemical Smog in China" campaign, from May 16th to June 5th, 2016 (see Fig. S1) (Hallquist et al., 2016). The PKUERS site is set on the roof at an academic building on the campus of Peking University in the northwest of Beijing. CP site is located on the fourth floor of a building on the Peking University Changping campus of Changping.

Four-channel samplers (TH-16A, Tianhong, China) consisting of three quartz filter channel and one Teflon filter channel, were employed to collect 12-h aerosol samples at PKUERS and CP, respectively. The sampling flow rate was 16.7 L min$^{-1}$. Teflon filters were weighed by a microbalance (Toledo AX105DR, USA) after a 24 h balance in an environmental controlled room (temperature $20 \pm 1^{o}C$, relative humidity $40 \pm 3\%$) for gravimetric analysis. Teflon-based samples were extracted by deionized water to measure water-soluble inorganic compounds (WSICs), namely $Na^+$, $NH_4^+$, $K^+$, $Mg^{2+}$, $Ca^{2+}$, $NO_3^-$, $SO_4^{2-}$ and $Cl^-$ by DIONEX ICS-2500 and ICS-2000 ion-chromatograph. One punch (1.45 cm$^2$) of quartz-based sample was then cut off to analyze the EC and OC via thermal-optical method using Sunset Laboratory-based instrument (NIOSH protocol, TOT). The other two quartz filters were then extracted and analyzed for chemical composition and particulate organic matters. Some daytime and nighttime samples were combined to ensure the detection of most organic compounds. To better understand the chemical speciation, daytime samples were separated from nighttime samples.

Authentic standards were used to identify and quantify the organic compounds. The analytical methods used in this study referred to the previous work (Song et al., 2014).

109    Briefly, the samples were first spiked with a mixture of internal standard, including

110    ketopinic acid (KPA), 20 kinds of deuterated compounds, and one carbon isotope

111    ^{13}C-substituted compound. The quartz filters were then ultrasonically extracted with

112    methanol: dichloromethane (v:v=1:3) solvent in water bath (temperature < 30 °C) for

113    3 times. Each time was 20 min. The extracts were filtered, and then concentrated

114    using a rotary vacuum evaporator. An ultra-pure nitrogen flow was used to further

115    concentrate the extracts into 0.5-1 ml. Each extracted solution was divided into two

116    portions, one of which added BSTFA (BSTFA/TMCS = 99:1, Supelco) to convert

117    polar organic compounds into trimethylsilanized derivatives. Afterwards, the

118    derivatized and the untreated samples were analyzed by an Agilent 6890 GC-MS

119    System (MSD GC-5973N) equipped with an Agilent DB-5MS GC column (30 m $\times$

120    0.25 mm $\times$ 0.5 μm).

121    **2.2 Source Apportionment**

122    A chemical mass balance modelling developed by the U.S. Environmental Protection

123    Agency (EPA CMB version 8.2) was applied to determine the apportion of the

124    primary contribution of OC (Schauer et al., 1996). This receptor model solved a set of

125    linear equations using ambient concentrations and chemical source profiles. CMB

126    approach depends strongly on the representativeness of the source profile. In this

127    study, five primary source profiles including vegetative detritus (Rogge et al., 1993),

128    coal combustion (Zheng et al., 2005), gasoline engines (Lough et al., 2007), diesel

129    engines (Lough et al., 2007) as well as biomass burning (Sheesley et al., 2007) were

130    input into the model. Fitting species including EC,n-alkanes, levoglucosan,

131    17β(H)-21α(H)-norhopane, 17α(H)-21β(H)-hopane, benzo(b)fluoranthene,

132    benzo(k)fluoranthene, benzo(e)pyrene, benzo(ghi)perylene, indeno(1,2,3-cd)pyrene.

133    The criteria for acceptable fitting results included the square regression coefficient of

134    the regression equation $R^2 > 0.85$ as well as the sum of square residual Chi-square

135    value $\chi^2 < 4$.

136     The tracer yield method was used to estimate the contributions of biogenic and

137     anthropogenic secondary organic aerosols using fixed tracers to SOC ratio ($f_{SOC}$)

138     based on laboratory experiments, which was $0.155 \pm 0.039$ for isoprene, $0.231 \pm 0.111$

139     for α-pinene, $0.0230 \pm 0.0046$ for β-caryophyllene and $0.0079 \pm 0.0026$ for toluene

140     (Kleindienst et al., 2007). The mass fraction depends on the degree of oxidation.

141     Besides, the uncertainty also depends on the selection of molecular tracers and the

142     simplified procedures by using single-valued mass fractions (Yttri et al., 2011; El

143     Haddad et al., 2011; Song et al., 2014; Guo et al., 2014b; Guo et al., 2014c). Previous

144     studies showed that SOA estimated by the tracer-yield method and POA apportioned

145     by CMB model could fully account for the OA in atmospheric atmosphere

146     (Lewandowski et al., 2008; Kleindienst et al., 2010). Besides, researchers found that

147     the total estimated SOC derived from tracer-yield method was in accordance with the

148     that stemmed from EC-tracer method during summer (Ding et al., 2012; Kleindienst

149     et al., 2010; Turpin and Huntzicker, 1995). Comparable results were also found

150     between tracer-yield method and positive matric factorization model (Hu et al., 2010;

151     Zhang et al., 2009). All these results firmly demonstrated that the tracer-yield method

152     is a valuable and convincing method to estimate the SOA contributions (X. Ding et al.,

153     2014).

154     Estimations based on boundary values were generally acknowledged to have the

155     largest source of uncertainties in the models, so those results could be used to

156     determine the possible limit of the estimations. Also, Kleindienst et al. carried out a

157     boundary analysis using the data from North California to measure the range of

158     estimated SOA contributions. Results revealed that the possible contributions of

159     isoprene, α-pinene, β-caryophyllene and toluene were within the scope of 70-130%,

160     50-220%, 70-120% and 60-160%, respectively. The above results were supposed to

161     be in the acceptable range for PM2.5 source apportionment. Besides, the standard

162     deviations of the tracer-to-SOC ratios were suitable as a source profile uncertainty

163     (Kleindienst et al., 2007). Despite the uncertainties above, tracer-yield represented a

## 3. Gaseous pollutants and particle chemical composition

### 3.1 Gaseous pollutants and meteorological conditions of the observation period

Mixing ratios of gaseous pollutants and meteorological conditions during the observation period were shown in Fig. S2 and Table S1. Compared with the results in summer of 2010 (Zheng et al., 2016a), the gaseous mixing ratios $SO_2$ and CO were lower than before owing to the desulfurization efforts made by the government. Higher concentrations of NO and $NO_2$ were caused by the increasing number of vehicles. The increment of ozone indicated the importance of secondary pollution. Clearly, ozone concentration at CP was higher than that of PKUERS while other pollutants were lower.

During the campaign, the average wind speed was low, showing average values of 2.3 $\pm 1.4$ m/s and 2.4 $\pm 1.5$ m/s at CP and PKUERS, respectively. The diurnal variations of wind directions and speeds are exhibited in Fig. S2. The prevailing wind was from south, with higher wind speed during the daytime.

To explore the influence of the air masses from different directions on fine particle loading and sources, back trajectory analysis was performed using National Oceanic and Atmospheric Administration (NOAA) Hybrid Single Particle Lagrangian Integrated Trajectory (HYSPLIT) model. We calculated 36 h air mass back trajectories arriving at two sampling site during the observation period using the HYSPIT-4 model with a $1\degree\times1\degree$ latitude-longitude grid and the final meteorological database. The model was run with the starting time of 0:00, 4:00, 8:00, 12:00, 16:00, and 20:00 UTC). The arrival level was set at 200 m above ground level. The method used in trajectory clustering was based on GIS-based software TrajStat (http://www.meteothinker.com/TrajStatProduct.aspx). 36-h back trajectories staring at 200 m above ground level in CP and PKUERS were calculated every 4 hours during

191 the entire campaign and then clustered according to their similarity in spatial

192 distribution using the HYSPLIT4 software. Three-cluster solution was adopted as

193 shown in Fig. S3. The three clusters were defined as Far North West (Cluster 1, Far

194 NW), Near West North (Cluster2, Near WN), and South (Cluster 3). South cluster was

195 found to be the most frequent one, accounting for 52% at CP and 64% at PKUERS.

196 Clusters Far NW and Near NW accounted for 17% and 31%, 17% and 19% at CP and

197 PKUERS, respectively.

198 **3.2 Overview of PM$_{2.5}$ chemical composition**

199 In this study, daily PM$_{2.5}$ concentrations fluctuated dramatically from 6.7 $\mu$g m$^{-3}$ to

200 80.3 $\mu$g m$^{-3}$ at CP, and from 9.6 to 82.5 $\mu$g m$^{-3}$ at PKUERS, respectively. A paired

201 t-test was used to compare the mass concentrations at two sites. The results indicate

202 that the mass concentrations showed statistically non-significant difference,

203 suggesting the regional particle pollution in Beijing. PM$_{2.5}$ mass concentrations during

204 the summer of 2008 to 2016 in Beijing are summarized in Table 1. Guo et al. (Guo et

205 al., 2013) reported the average PM$_{2.5}$ concentrations during the summers of 2000 to

206 2008, which showed distinct decreasing tendency during 2000-2006 and then slightly

207 increased in 2007 due to unfavorable meteorological conditions. To better understand

208 the variation tendency of the PM$_{2.5}$ in the summer of Beijing, we compared the fine

209 particle matter data since 2008. Compared with 2008, the PM$_{2.5}$ concentrations

210 decreased from 92.3 $\pm$ 44.7 $\mu$g m$^{-3}$ to 88.2 $\mu$g m$^{-3}$ in 2009 and 62.7 $\mu$g m$^{-3}$ in 2010.

211 The mass concentration continued falling to 45.5 $\mu$g m$^{-3}$ in 2016. This decreasing is

212 attributed to the drastic emission control measures implemented by the Beijing

213 government since 2012. In spite of the prominent decrease of the PM$_{2.5}$ mass

214 concentrations, the aerosol loading in Beijing was still much higher than that in

215 developed countries (Tai et al., 2010; Barmpadimos et al., 2012; Park and Cho, 2011).

216 Fig. S4 showed the chemical composition of PM$_{2.5}$. In general, organic particulate

217 matters (OM, OC*1.6) and sulfate were the two dominant components, accounting for

218      more than 50% of the $PM_{2.5}$ mass concentration during the field campaign. The

219      average concentration of total WSICs for CP was 17.4 $\pm$ 11.5 μg m$^{-3}$, higher than that

220      of PKUERS (12.2 $\pm$ 8.5μg m$^{-3}$). Among the WSICs, secondary inorganic ions (sulfate,

221      nitrate, and ammonium) were the most abundant compounds, indicating secondary

222      particles played great roles in the summer of Beijing. The higher sulfate proportion

223      could be explained by the increased photochemical conversion of sulfur dioxide to

224      sulfate aerosol (Xiang et al., 2017). Relevant data of main WSICs (sulfate, nitrate and

225      ammonia) during 2008 to 2016 were also included in table 1 to better elucidate the

226      drastic decrease of fine particulate matter in recent years. Results showed that the

227      daily average concentration of WSICs decreased from 2008 to 2016, with sulfate

228      decreased from 35.6 μg/m$^3$ to 4.7 μg/m$^3$, nitrate decreased from 7.9 μg/m$^3$ to 2.4

229      μg/m$^3$, ammonia decreased from 15.2 μg/m$^3$ to 3.5 μg/m$^3$. The significant decrease of

230      WSICs confirmed the effectiveness of the control measures taken by the government.

231      Carbonaceous aerosols, i.e. organic carbon (OC) and elemental carbon (EC) were also

232      great contributors to $PM_{2.5}$ concentrations. Higher proportion of OC and EC at

233      PKUERS demonstrated severe carbonaceous pollution in urban Beijing, which might

234      have close correlation with the higher traffic flow, coal/wood combustion by residents

235      and industrial emissions (Wang et al., 2006; Dan et al., 2004; Cao et al., 2004).

236      Comparison of the OC, EC concentrations from 2008 to 2016 were also listed in Table

237      1. Unlike $PM_{2.5}$, OC concentration at PKUERS showed a higher OC concentration

238      (11.0 $\pm$ 3.7 μg m$^{-3}$) compared with that in 2008 (9.2 $\pm$ 3.3μg m$^{-3}$), suggesting organic

239      aerosol pollution becomes more and more important. EC concentration decreased

240      dramatically to 0.7 $\pm$ 0.5 μg m$^{-3}$ at CP and 1.8 $\pm$ 1.0 μg m$^{-3}$ at PKUERS, which

241      showed the lowest value since 2000. This could be attributed to the implementation of

242      air pollution prevention and control action plan enacted by the state council since

243      2013. Therefore, we could draw a conclusion that the drastic decrease of fine

244      particulate matter in Beijing was mainly due to the well-controlled EC and WSICs,

245      with negligible contribution of OC.

246 To evaluate the influences of the air masses from different directions on the $PM_{2.5}$

247 loadings during the campaign, three categories were divided according to the back

248 trajectory clustering analysis (See Fig. S5). In general, cluster south represented the

249 most polluted air mass origin followed by clusters Near WN and Far NW, which was

250 in accordance with previous studies demonstrating severe aerosol pollution in

251 southerly air flow in summer of Beijing (Huang et al., 2010; Sun et al., 2010).

252 **3.3 Concentration of particulate organic species from different air mass origins**

253 The organic species (except secondary organic tracers) were divided into 12

254 categories. Their concentrations in different directions according to the back trajectory

255 clustering were shown in Fig. S6. Detailed information for each class at the two sites

256 could be found in the supplementary material (Fig. S7). Cluster south showed higher

257 particulate organic matter concentration, followed by cluster near WN and far NW,

258 indicating more severe aerosol pollution from the south. Our result consists with the

259 previous studies that more pollution emissions are from the south area of Beijing than

260 those from the north (Wu et al., 2011; Zhang et al., 2009).

261 For all the species, the histogram showed the daily average concentrations with error

262 bars representing one standard deviation. Dicarboxylic acid was the most abundant

263 species among all the components, demonstrating the great contribution of the

264 secondary formation to the organic aerosols in the summer of Beijing (Guo et al.,

265 2010). A series of n-alkanes ranging from C12 to C36 were analyzed. Their

266 distribution during the observation period was shown in Fig. S7 (a). The

267 maximum-alkane concentration species ($C_{max}$) were C27 and C29. The odd carbon

268 preference was an indicative of biogenic sources (vegetative matters and biomass

269 burning) (Huang et al., 2006; Rogge et al., 1993). In this study, total PAHs were much

270 lower than previous studies in summer of Beijing, suggesting the effectiveness of the

271 control strategies since 2013 (Wang et al., 2009). According to Fig. S7 (c), five ring

272 PAHs were dominant species among all the species, followed by four-ring and

273  six-ring PAHs. In total, four to six ring PAHs had higher abundancy, accounting for

274  more than 60% of the total PAHs. The result was much similar with previous studies

275  that the distribution of PAHs was impacted by the volatility of PAHs and the

276  temperature (Wang et al., 2009; Guo et al., 2013). Saccharide was considered to

277  originate from biomass burning (Simoneit et al., 1999). In this study, we quantified

278  three sugar compounds including levoglucosan, manosan and galactosan, in which

279  levoglucosan was considered as a good tracer for biomass burning. The average daily

280  mass concentration of levoglucosan at CP and PKUERS were $53.03 \pm 39.26$ ng m$^{-3}$

281  and $59.87 \pm 38.93$ ng m$^{-3}$, respectively. It's worth mentioning that the levoglucosan

282  concentration was the lowest in recent years (Cheng et al., 2013; Guo et al., 2013).

283  Hopanes have been considered as markers for oil combustion (Lambe et al., 2009),

284  vehicles (i.e. gasoline-powered and diesel-powered engine) (Cass, 1998; Lough et al.,

285  2007) and coal combustion (Oros and Simoneit, 2000). Nevertheless, contributions of

286  coal combustion to hopanes were much less than that of vehicle exhaustion.

287  Concentrations of quantified hopanes including 17α(H)-22,29,30-trishopane,

288  17β(H)-21α(H)-norhopane, and 17α(H)-21β(H)-hopane of CP and PKUERS are

289  shown in Fig. S7(d). The total average concentrations of hopanes were $3.05 \pm 1.53$ ng

290  m$^{-3}$ for CP and $3.90 \pm 2.06$ ng m$^{-3}$ for PKUERS. The daily averaged hopanes

291  concentrations at urban site PKUERS were much higher than that of CP, which could

292  probably explained by the heavier vehicle emissions in the urban area. The

293  concentrations of primary organic tracers used in CMB model were listed in Table S2.

294  **3.4 Biogenic and anthropogenic SOA tracers**

295  Table S3 compared the SOA tracers measured in this work with those in other regions

296  in the world as well as that observed in Beijing 2008. The sites for comparison

297  include an urban background site at Indian Institute of Technology Bombay, Mumbai,

298  India (IITB) (Fu et al., 2016), an outflow region of Asian aerosols and precursors

299  Cape Hedo, Okinawa, Japan (CH) (Zhu et al., 2016), a residential site at Yuen Long,

300  Hong Kong (YL) (Hu et al., 2008), three industrial sites at Cleveland Ohio (CL, data

301 was averaged among the three sites), a suburban site in the Research Triangle Park
302 North California (RTP). The detailed information about these sites were summarized
303 in the supplementary material.

304 Three isoprene-SOA tracers i.e. two 2-methyltetrols (2-methyltheitol and
305 2-methylerythritol) and 2-methylglyceric acid were detected. The summed
306 concentration of the isoprene-SOA tracers ranged from 3.7 to 62.3 ng m$^{-3}$ at CP and
307 8.6 to 46.5 ng m$^{-3}$ at PKUERS. The concentration was higher than that of IITB and
308 CH. Compared with the isoprene-SOA tracers in 2008, the concentrations in 2016
309 were lower.

310 Nine α-pinene tracers were identified. The sum of the tracers ranged from 20.9 to
311 282.3 ng m$^{-3}$ at CP and 50.0 to 161.4 ng m$^{-3}$ at PKUERS, which had similar
312 distribution pattern with that measured in 2008 Beijing and YL. The total α-pinene
313 tracer concentrations were lower than those in 2008, while still much higher than the
314 concentrations in other regions of the world.

315 β-caryophyllinic acid is one of the oxidation products of β-caryophyllene which is
316 considered as a tracer for β-caryophyllene SOA. In this study, β-caryophyllinic acid
317 concentrations ranged from 1.4 to 16.7 ng m$^{-3}$ at CP, and 0.9 to 12.0 ng m$^{-3}$ at
318 PKUERS, with average daily average concentrations of 6.1 ±3.5 ng m$^{-3}$ and 6.0 ±2.8
319 ng m$^{-3}$ for CP and PKUERS, respectively. The values were lower than those at YL and
320 RPT, higher than that measured at Yufa and PKUERS in 2008.

321 2,3-Dihydroxy-4-oxopentanoic acid is deemed as a tracer for toluene SOA. Our
322 results showed that the 2,3-Dihydroxy-4-oxopentanoic acid concentration was 9.7 ±
323 7.3 ng m$^{-3}$ at CP and 11.0 ±3.7 ng m$^{-3}$ at PKUERS. Compared with other regions of
324 the world, the concentrations of 2,3-Dihydroxy-4-oxopentanoic acid was much higher,
325 implying higher contributions of anthropogenic sources at Beijing. However, the
326 2,3-dihydroxy-4-oxopentanoic acid concentrations in CP were lower than that of
327 PKUERS.

## 4. Primary sources and secondary formation of organic aerosols

**4.1 Contributions of primary and secondary organic aerosols**

A CMB model and the tracer-yield method were used to quantify the contributions of primary and secondary sources to the ambient organic carbon (See Fig. 1). On average, the primary sources accounted for 42.6 ± 15.4% and 50.4 ± 19.1% of the measured OC at CP and PKUERS, respectively. The vehicle emissions were the dominant primary sources, with the contributions of 28.8 ± 14.8% and 37.6 ± 19.3% at PKUERS and CP, respectively, implying the urgency to control vehicular exhaustion in urban areas. Despite of the lower contribution of the gasoline exhaust at PKUERS, the mass concentration of the gasoline exhaust was higher compared with that of CP given the higher OC loading at PKUERS. The contributions of biomass burning were 3.9 ± 2.6% and 5.0 ± 2.2% at CP and PKUERS, respectively, showing the higher concentrations at night. The drastic change of the biomass burning contribution in CP at night was due to occasional burning activities at night. Coal combustion contributed 5.8 ± 5.5% and 4.6 ± 2.6% of the measured OC at CP and PKUERS. The higher contribution at CP was due to more burning activities in the suburban areas.

The secondary organic sources accounted for 20.2 ± 6.7% of the organic carbon at CP, with 1.6 ± 0.4% from isoprene, 4.4 ± 1.5% from α-pinene, 2.7 ± 1.0% from β-caryophyllene and 12.5 ± 3.4% from toluene. As for PKUERS, the secondary organic sources took up 30.5 ± 12.0% of the measured OC, in which isoprene was responsible for 2.3 ± 0.9%, α-pinene for 5.6 ± 1.9%, β-caryophyllene for 3.6 ± 2.6% and toluene for 19.0 ± 8.2%. Haque et al. (Haque et al., 2016) used tracer-based method to apportion the organic carbon and results showed that the biogenic SOC was responsible for 21.3% of the total OC with isoprene SOC contributing 17.4%, α/β-pinene SOC contributing 2.5% and β-caryophyllene SOC contributing 1.4% in the summer of Alaska, implying the significant contributions of the biogenic SOA to the

355 loading of the organic aerosol. Our results exhibited that the biogenic SOA

356 concentration was comparable or even high than that at some forest sites in other

357 places of the world (Miyazaki et al., 2012; Stone et al., 2012; Claeys et al., 2004;

358 Kourtchev et al., 2008). The SOA formation mechanism is complicated. A possible

359 reason is the high oxidation capacity in China. Higher oxidation capacity in China

360 may fasten the chemical lifetime of reactive gases and accelerate the aerosol aging

361 process which leads to an increase in biogenic SOA (Ghirardo et al., 2016). Another

362 possible reason derived from the complicated emissions of anthropogenic VOCs

363 which can lead to an enhancement of secondary organic aerosol formation from

364 biogenic precursors (Hoyle et al., 2011). We also compare the isoprene concentration

365 with the forest site according to some literatures. Wang et al. (Wang et al., 2010)

366 discovered that the mean isoprene concentration was 0.24 ppbv at PKUERS in June

367 2008. Lappalainen et al. (Lappalainen et al., 2009) measured the isoprene

368 concentration of the boreal forest in Hyytiala and found that the mean concentration

369 of isoprene was 0.15 ppbv. This comparable, or even higher concentration of isoprene

370 may be due to different sources of biogenic VOCs. More work is still needed to

371 investigate the SOA formation mechanism under Air Pollution Complex in China.

372 Stone et al. (Stone et al., 2009) discovered that primary and secondary sources

373 accounted for $83 \pm 8\%$ of the measured organic carbon, with primary sources

374 accounted for $37 \pm 2\%$ and SOC contributed for $46 \pm 6\%$ with $16 \pm 2\%$ from biogenic

375 gas-phase precursors and $30 \pm 4\%$ from toluene using CMB model and tracer-based

376 method at Cleveland with heavy industries, implying that anthropogenic sources

377 played great roles in the formation of SOA. Our results showed a similar with the

378 results published by Stone et al., where anthropogenic sources i.e. toluene derived

379 SOC dominated the apportioned SOC. Our research revealed an important point that

380 controlling SOA seems feasible in the developing countries like China. It is difficult

381 to control SOA in developed countries, since biogenic SOA are dominant. However,

382 deducting anthropogenic precursors may be an efficient way to reduce the SOA

383  pollution where anthropogenic SOA is dominant. On average, 62.8 ± 18.3% and 80.9

384  ± 27.2% of the measured OC were apportioned at CP and PKUERS, respectively.

385  About 36.3 ± 18.1% and 29.3 ± 15.6% of the OC sources remained unknown, which

386  were probably composed of uncharacterized primary or secondary sources. Further

387  research is needed to explain the unapportioned sources of OC.

388  Due to the drastic emission control measures taken by the Beijing government, the

389  primary and secondary sources in Beijing may change greatly. Fig. 2 displayed the

390  comparison of the sources between 2008 and 2016 at the same site PKUERS. We

391  compared the average contributions by percentage rather than the mass concentration.

392  In general, primary sources contributed 50.4 ± 19.1% of the measured OC in 2016,

393  closely correlated to the increasing contribution of vehicular emissions. Gasoline

394  engines accounted for 18% of the measured OC, showing an enhancement of 80%

395  with respect to 2008. This might be related to the rising number of the vehicles in

396  Beijing. In comparison, diesel exhaust decreased by 12.5% due to the strict control

397  measures made by the government. A 28.5% and 20% reduction of coal combustion

398  and biomass burning could also be found due to the drastic measures made by the

399  government. Compared with 2008, contributions of secondary organic aerosol

400  decreased by 29.4%, in which biogenic SOC served as the biggest contributor to this

401  decreasing. The formation of biogenic SOA is complicated. Several factors can affect

402  biogenic SOC formation, among which the precursor concentration is one of the

403  crucial factors. Biogenic VOCs, i.e. isoprene, α-pinene etc. are predominantly emitted

404  from plant foliage in a constitutive manner. The emission rate of biogenic VOCs

405  depends on various factors, e.g. radiation, temperature, humidity, meteorological

406  conditions and seasonality (Ghirardo et al., 2016). Two or more of them will act

407  synergistically to have an effect on the concentration of isoprene SOC. Besides, the

408  changes of the vegetation in certain area may also play a part in the change of the

409  SOC concentration. Considering its comprehensive synergistic effect, it's difficult to

410  determine the main reason responsible for the isoprene SOC decrease.

411     However, the contribution of toluene SOC was the highest among the apportioned

412     SOC, which was different from the results of the most developed countries in the

413     world. Compared with previous studies, except β-caryophyllene SOC, vegetative

414     detritus and gasoline exhausts, the contributions of all other sources decreased, e.g.

415     isoprene SOC, α-pinene SOC, toluene SOC, biomass burning, diesel exhaust, and coal

416     combustion.   However, the increases in β-caryophellene SOC, vegetative detritus

417     and gasoline exhausts could not compensate for the decreases of other sources. This

418     can be attributed to the larger portion of uncharacterized sources compared with 2008.

419     The uncharacterized sources may mainly contain cooking emissions, mineral and road

420     dust, industrial pollution as well as other uncharacterized secondary sources (Tian et

421     al., 2016; Liu et al., 2016). In summary, the contributions of most POA decreased in

422     recent years, except for gasoline exhaust, indicating more efforts should be made to

423     control the gasoline emission. The apportioned SOC was also decreased with toluene

424     SOC served as the dominant source. Our results revealed that deducting

425     anthropogenic precursors may be an efficient way to control SOA pollution in China.

426     **4.2 Organic aerosol sources from different air mass origins**

427     The regional sources and transport of air pollutants exert profound impacts on air

428     quality of Beijing. To better understand the regional impacts on the primary and

429     secondary aerosol sources of Beijing, source apportionment results when air mass

430     from different origins were shown in Fig. 3. Vehicular emissions i.e. gasoline and

431     diesel exhaust showed identical contributions from different air mass origins (31.0%

432     from south vs 31.3% from Near WN vs 31.7% from Far NW) at PKUERS,

433     demonstrating the vehicular pollution could mostly be attributed to the vehicular

434     emission at the local site. However, the contribution of vehicular emission at CP

435     showed significant difference from different air mass origins, with lowest contribution

436     when air mass was from far northwest. This might be explained by regional transport

437     from different directions. Comparable contributions of coal combustion and biomass

438     burning were found at CP and PKUERS from different air mass origins, implying the

439    regional pollution in Beijing. Similarly, biogenic SOC showed similar contributions

440    from different air mass origins both at the regional site and the urban site. From all the

441    directions, the toluene SOC (anthropogenic source) was the largest contributor to

442    apportioned SOC, with higher concentrations at the urban site PKUERS. On the

443    whole, most of the sources showed comparable contribution from different air mass

444    origins, implying the pollution in Beijing was regional.

445    **4.3 Influencing factors for secondary organic aerosol formation in the summer of**

446    **Beijing**

447    Laboratory experiments have revealed that several factors can influence the SOA

448    formation, e.g. oxidants (OH radical, ozone etc.), temperature, humidity, particle

449    water content and acidity. We found that the correlations between SOC and

450    ozone/temperature are different for daytime and nighttime samples. However, it's not

451    significant for water content and hydrogen ions concentration. Therefore, we separate

452    the data between day and night between SOC and ozone/temperature, and use entire

453    data for the analysis of particle water and acidity. In this work, the relationships

454    between estimated SOA and these factors were investigated to better understand the

455    SOA formation in Beijing.

456    **SOA formation from ozonolysis**

457    Ozone is considered as an important oxidant for SOA formation. Fig. 4 (a)(b) showed

458    the correlation with ozone mixing ratio and SOC. It is clear that SOC increased

459    significantly with the increasing of ozone mixing ratio, which is consistent with

460    previous studies in Beijing (Guo et al. 2012). Different correlations were found

461    between day and night samples, with better correlation for the daytime samples at

462    both sites, implying SOA may have other formation mechanism at night other than

463    ozonolysis. At CP, the growth rate of SOC with $O_3$ was similar for day and night

464    samples, which was 0.02 μg m$^{-3}$ per ppbv ozone. For PKUERS, the increment rate of

465    the SOC towards ozone was 0.04 $\mu g\ m^{-3}$ and 0.02 $\mu g\ m^{-3}$ per ppbv ozone at day and

466    night, respectively.

**Influence of temperature and relative humidity on SOA formation**

468    Temperature was considered as a great influencing factor on SOA formation. On the

469    one hand, higher temperature promoted the evaporation of the semi volatile SOA. On

470    the other hand, high-temperature conditions would favor the oxidation, which would

471    accelerate the SOA formation (Saathoff et al., 2009). Fig. 4 (c) (d) showed the

472    variation of SOC concentrations with the temperature. In this study, SOC

473    concentration showed positive correlation with temperature at CP and PKUERS,

474    demonstrating that temperature favors the SOA formation in the summer of Beijing.

475    Moreover, different correlation of the day and the night samples imply the different

476    pathways of SOA formation. However, poor relations could be found between SOC

477    and RH.

**Effects of aqueous-phase acid catalyzed reactions on SOA formation**

479    Aerosol water and acidity have been considered to have great impact on the

480    aqueous-phase SOA formation (Cheng et al., 2016). To figure out the influences of

481    water content and aerosol acidity on the aqueous-phase reactions, ISORROPIA-II

482    thermodynamic equilibrium model was used (Surratt et al., 2007). The model was set

483    at forward mode, based on the concentrations of particle phase $Na^+$, $NH_4^+$, $K^+$, $Mg^{2+}$,

484    $Ca^{2+}$, $NO_3^-$, $SO_4^{2-}$, $Cl^-$ and gaseous $NH_3$ as well as ambient temperature and RH.

485    Results showed that the average aerosol water content at CP was 3.87 $\pm$ 3.73 $\mu g\ m^{-3}$,

486    higher than that at PKUERS (1.83 $\pm$ 1.81 $\mu g\ m^{-3}$). The water content was lower in

487    2016 than that in 2008. The estimated SOC concentration showed good correlations

488    with water content at both sites. Compared with CP, the correlation factor in PKUERS

489    was better, implying that aqueous phase reaction may be more important in the urban

490    area. Different correlation could be found at different liquid water contents, especially

491    for CP, where liquid water contented spanned a wide range, implying that different

492    mechanisms may exist at different liquid water content.

493    In this study, modeled $H^+$ concentration and SOC showed significant correlation

494    ($p < 0.05$) at the two places, which indicated that acid-catalyzed reaction might provide

495    a crucial pathway for the SOA formation in the summer of Beijing. Laboratory studies

496    showed that acid-catalyzed reactive uptake might play great role in the enhancement

497    of SOA (Zhang et al., 2014; Surratt et al., 2010; Jang et al., 2002). However, contrary

498    conclusions were made by other group, demonstrating the inconsistence of the aerosol

499    acidity and the SOA formation (Wong et al., 2015; Kristensen et al., 2014). The

500    contradiction might give the facts that the impacts of the acidity on the SOA loading

501    varied from place to place, determined by the specific environmental conditions.

502    Linear regression showed that the enhancement of SOC with modeled $H^+$

503    concentration were at a value of 0.02 $\mu g\ m^{-3}$ per nmol $H^+$, which was lower than the

504    previous results (0.046 for PKUERS, and 0.041 for Yufa, 2008). Offenberg et al.

505    (Offenberg et al., 2009) discovered good correlation between SOC and $[H^+]_{air}$, with

506    $R^2$ value of 0.815. Besides, a one nmol $m^{-3}$ $[H^+]_{air}$ would give rise to 0.015 $\mu g\ m^{-3}$

507    SOC increase from the oxidation of α-pinene in the chamber experiment. We also

508    analyzed the relationship between apportioned SOC and sulfate concentration and

509    found that the apportioned SOC increased with the increase of sulfate concentration.

510    The coefficient $R^2$ were 0.41 and 0.45 for CP and PKUERS, respectively, indicating

511    that the increase of SOC may be influenced by the sulfate aerosol. As such, the

512    increase in SOC is likely arise from the acid-catalyzed reactions with the participation

513    of sulfate aerosols. In the present work, different correlations could be found at

514    different modeled $H^+$ concentrations where apportioned SOC increased significantly

515    as the $H^+$ concentration increased and then increased slowly at a certain level,

516    showing gradient growth at different hydrogen-ion concentrations. Therefore, aqueous

517    phase acid-catalyzed reactions may influence the SOA formation through different

518    mechanisms at varied level of liquid water concentration and aerosol acidity.

## 5. Conclusion

High concentrations of fine particles were observed during the "Campaign on Photochemical Smog in China", with the average mass concentrations of 45.48 ± 19.78 μg m$^{-3}$ and 42.99 ± 17.50 μg m$^{-3}$, at CP site and PKUERS site, respectively. Compared with previous studies, the concentrations of $PM_{2.5}$, EC and estimated SOC decreased significantly, due to the drastic measures implemented by the government in the recent years. However, OC showed a higher concentration, suggesting particulate organic matters become more and more important in Beijing. CMB modeling and tracer-yield method were used to apportion the primary and secondary organic aerosol sources. The apportioned primary and secondary OC accounted for 62.8 ± 18.3% and 80.9 ± 27.2% of the measured OC at CP and PKUERS, respectively. Vehicle emissions i.e. diesel and gasoline engine emissions were the major primary organic aerosol sources, which contributed to 28.8 ± 14.8% and 37.6 ± 19.3% of the OC at CP and PKUERS, respectively. Compared with the results of the previous work, the gasoline engine emission contributed almost twice of that in 2008 (18.0% vs 10.0%), while the contribution of diesel engine emission decreased by 12.5% compared with the result in 2008. Besides, the contributions of biomass burning and coal combustion both decreased. The apportioned biogenic and anthropogenic SOC can explain 20.2 ± 6.7% and 30.5 ± 12.0% of the measured OC at CP and PKUERS, respectively. The contribution of toluene SOC is the highest among the apportioned SOC, which is different from the results of the most developed countries in the world. Our results revealed an important point, which is that controlling SOA seems feasible in the developing countries like China. It is difficult to control SOA in developed countries, since biogenic SOA are dominant. However, deducting anthropogenic precursors may be an efficient way to reduce the SOA pollution where anthropogenic SOA is dominant. Back trajectory clustering analysis showed that the particle source contributions were similar when air masses were from different directions, suggesting the regional organic particle pollution in Beijing. However, the higher organic particle

547    loading from south cluster indicates that there were more emissions from southern

548    region of Beijing. The present work also implied that the aqueous phase

549    acid-catalyzed reactions may be an important SOA formation mechanism in summer

550    of Beijing.

## Acknowledgement

551

552    This research is supported by the National Key R&D Program of China

553    (2016YFC0202000, Task 3), the National Natural Science Foundation of China

554    (21677002), framework research program on 'Photochemical smog in China' financed

555    by Swedish Research Council (639-2013-6917).

# References

Barmpadimos, I., Keller, J., Oderbolz, D., Hueglin, C., and Prévôt, A.: One decade of parallel fine ($PM_{2.5}$) and coarse ($PM_{10}$–$PM_{2.5}$) particulate matter measurements in Europe: trends and variability, Atmos Chem Phys, 12, 3189-3203, 2012.

Cao, J. J., Lee, S. C., Ho, K. F., Zou, S. C., Fung, K., Li, Y., Watson, J. G., and Chow, J. C.: Spatial and seasonal variations of atmospheric organic carbon and elemental carbon in Pearl River Delta Region, China, Atmospheric Environment, 38, 444t-4456, http://doi.org/10.1016/j.atmosenv.2004.05.016, 2004.

Cass, G. R.: Organic molecular tracers for particulate air pollution sources, Trac-Trends in Analytical Chemistry, 17, 356-366, 10.1016/s0165-9936(98)00040-5, 1998.

Cheng, Y., Engling, G., He, K. B., and Duan, F. K.: Biomass burning contribution to Beijing aerosol, Atmospheric Chemistry & Physics, 13, 7765-7781, 2013.

Cheng, Y., Zheng, G., Wei, C., Mu, Q., Zheng, B., Wang, Z., Gao, M., Zhang, Q., He, K., and Carmichael, G.: Reactive nitrogen chemistry in aerosol water as a source of sulfate during haze events in China, Science Advances, 2, e1601530, 2016.

Claeys, M., Graham, B., Vas, G., Wang, W., Vermeylen, R., Pashynska, V., Cafmeyer, J., Guyon, P., Andreae, M. O., and Artaxo, P.: Formation of Secondary Organic Aerosols Through Photooxidation of Isoprene, Science, 303, 1173, 2004.

Dan, M., Zhuang, G., Li, X., Tao, H., and Zhuang, Y.: The characteristics of carbonaceous species and their sources in PM2.5 in Beijing, Atmospheric Environment, 38, 3443-3452, http://doi.org/10.1016/j.atmosenv.2004.02.052, 2004.

Ding, X., Wang, X. M., Gao, B., Fu, X. X., He, Q. F., Zhao, X. Y., Yu, J. Z., and Zheng, M.: Tracer‐based estimation of secondary organic carbon in the Pearl River Delta, south China, Journal of Geophysical Research Atmospheres, 117, 2012.

583    Ding, X., He, Q. F., Shen, R. Q., Yu, Q. Q., and Wang, X. M.: Spatial distributions of
584        secondary organic aerosols from isoprene, monoterpenes, beta-caryophyllene,
585        and aromatics over China during summer, Journal of Geophysical
586        Research-Atmospheres, 119, 11877-11891, 10.1002/2014jd021748, 2014.

587    El Haddad, I., Marchand, N., Temime-Roussel, B., Wortham, H., Piot, C., Besombes,
588        J. L., Baduel, C., Voisin, D., Armengaud, A., and Jaffrezo, J. L.: Insights into the
589        secondary fraction of the organic aerosol in a Mediterranean urban area:
590        Marseille, Atmos Chem Phys, 11, 2059-2079, 2011.

591    Fu, P., Aggarwal, S. G., Chen, J., Li, J., Sun, Y., Wang, Z., Chen, H., Liao, H., Ding,
592        A., Umarji, G. S., Patil, R. S., Chen, Q., and Kawamura, K.: Molecular Markers
593        of Secondary Organic Aerosol in Mumbai, India, Environ. Sci. Technol., 50,
594        4659-4667, 10.1021/acs.est.6b00372, 2016.

595    Gao, J. J., Tian, H. Z., Cheng, K., Lu, L., Wang, Y. X., Wu, Y., Zhu, C. Y., Liu, K. Y.,
596        Zhou, J. R., Liu, X. G., Chen, J., and Hao, J. M.: Seasonal and spatial variation
597        of trace elements in multi-size airborne particulate matters of Beijing, China:
598        Mass concentration, enrichment characteristics, source apportionment, chemical
599        speciation and bioavailability, Atmospheric Environment, 99, 257-265,
600        10.1016/j.atmosenv.2014.08.081, 2014.

601    Ghirardo, A., J. Xie, X. Zheng, Y. Wang, R. Grote, K. Block, J. Wildt, T. Mentel, A.
602        Kiendler-Scharr, and M. Hallquist (2016), Urban stress-induced biogenic VOC
603        emissions and SOA-forming potentials in Beijing, Atmospheric chemistry and
604        physics, 16(5), 2901-2920.

605    Guo, S., Hu, M., Wang, Z. B., Slanina, J., and Zhao, Y. L.: Size-resolved aerosol
606        water-soluble ionic compositions in the summer of Beijing: implication of
607        regional secondary formation, Atmos Chem Phys, 10, 947-959, 2010.

608    Guo, S., Hu, M., Guo, Q., Zhang, X., Zheng, M., Zheng, J., Chang, C. C., Schauer, J.
609        J., and Zhang, R.: Primary Sources and Secondary Formation of Organic

Aerosols in Beijing, China, Environmental Science & Technology, 46, 9846-9853, 10.1021/es20425641, 2012.

Guo, S., Hu, M., Guo, Q., Zhang, X., Schauer, J., and Zhang, R.: Quantitative evaluation of emission controls on primary and secondary organic aerosol sources during Beijing 2008 Olympics, Atmos Chem Phys, 13, 8303-8314, 2013.

Guo, S., Hu, M., Zamora, M. L., Peng, J., Shang, D., Zheng, J., Du, Z., Wu, Z., Shao, M., and Zeng, L.: Elucidating severe urban haze formation in China, Proceedings of the National Academy of Sciences, 111, 17373-17378, 2014a.

Guo, S., Hu, M., Guo, Q. F., and Shang, D. J.: Comparison of Secondary Organic Aerosol Estimation Methods, Acta Chim Sinica, 72, 658-666, 10.6023/A14040254, 2014b.

Guo, S., Hu, M., Shang, D., Guo, Q., and Hu, W.: Research on Secondary Organic Aerosols Basing on Field Measurement, Acta Chim. Sinica, 72, 145-157, DOI: 10.6023/A13111169, 2014c.

Haque, M. M., Kawamura, K., and Kim, Y.: Seasonal variations of biogenic secondary organic aerosol tracers in ambient aerosols from Alaska, Atmospheric Environment, 130, 95-104, 10.1016/j.atmosenv.2015.09.075, 2016.

Hoyle, C., Boy, M., Donahue, N., Fry, J., Glasius, M., Guenther, A., Hallar, A., Huff Hartz, K., Petters, M., and Petäjä, T.: A review of the anthropogenic influence on biogenic secondary organic aerosol, Atmospheric Chemistry and Physics, 11, 321-343, 2011.

Hu, D., Bian, Q., Li, T. W., Lau, A. K., and Yu, J. Z.: Contributions of isoprene, monoterpenes, β‐caryophyllene, and toluene to secondary organic aerosols in Hong Kong during the summer of 2006, Journal of Geophysical Research: Atmospheres, 113, 2008.

Hu, D., Bian, Q., Lau, A. K. H., and Yu, J. Z.: Source apportioning of primary and secondary organic carbon in summer PM2.5 in Hong Kong using positive matrix

factorization of secondary and primary organic tracer data, Journal of Geophysical Research Atmospheres, 115, 2010

Hu, M., Guo, S., Peng, J.-f., and Wu, Z.-j.: Insight into characteristics and sources of PM2. 5 in the Beijing–Tianjin–Hebei region, China, National Science Review, 2, 257-258, 2015.

Huang, X.-F., He, L.-Y., Hu, M., and Zhang, Y.-H.: Annual variation of particulate organic compounds in PM 2.5 in the urban atmosphere of Beijing, Atmospheric Environment, 40, 2449-2458, 2006.

Huang, X. F., He, L. Y., Hu, M., Canagaratna, M. R., Sun, Y., Zhang, Q., Zhu, T., Xue, L., Zeng, L. W., and Liu, X. G.: Highly time-resolved chemical characterization of atmospheric submicron particles during 2008 Beijing Olympic Games using an Aerodyne High-Resolution Aerosol Mass Spectrometer, Atmospheric Chemistry & Physics Discussions, 10, 8933-8945, 2010.

Jang, M. S., Czoschke, N. M., Lee, S., and Kamens, R. M.: Heterogeneous atmospheric aerosol production by acid-catalyzed particle-phase reactions, Science, 298, 814-817, 10.1126/science.1075798, 2002.

Kleindienst, T. E., Jaoui, M., Lewandowski, M., Offenberg, J. H., Lewis, C. W., Bhave, P. V., and Edney, E. O.: Estimates of the contributions of biogenic and anthropogenic hydrocarbons to secondary organic aerosol at a southeastern US location, Atmospheric Environment, 41, 8288-8300, 2007.

Kleindienst, T., MichaelLewandowski, Offenberg, J., Edney, E., MohammedJaoui, MeiZheng, XiangDing, and Edgerton, E.: Contribution of Primary and Secondary Sources to Organic Aerosol and PM2.5 at SEARCH Network Sites, Journal of the Air & Waste Management Association, 60, 1388, 2010.

Kourtchev, I., Warnke, J., Maenhaut, W., Hoffmann, T., and Claeys, M.: Polar organic marker compounds in PM2.5 aerosol from a mixed forest site in western Germany, Chemosphere, 73, 1308-1314, 2008.

664 Kristensen, K., Cui, T., Zhang, H., Gold, A., Glasius, M., and Surratt, J.: Dimers in

665         α-pinene secondary organic aerosol: effect of hydroxyl radical, ozone, relative

666         humidity and aerosol acidity, Atmos Chem Phys, 14, 4201-4218, 2014.

667 Lambe, A. T., Miracolo, M. A., Hennigan, C. J., Robinson, A. L., and Donahue, N. M.:

668         Effective Rate Constants and Uptake Coefficients for the Reactions of Organic

669         Molecular Markers (n-Alkanes, Hopanes, and Steranes) in Motor Oil and Diesel

670         Primary Organic Aerosols with Hydroxyl Radicals, Environ. Sci. Technol., 43,

671         8794-8800, 10.1021/es901745h, 2009.

672 Lappalainen, H., Sevanto, S., Bäck, J., Ruuskanen, T., Kolari, P., Taipale, R., Rinne, J.,

673         Kulmala, M., and Hari, P.: Day-time concentrations of biogenic volatile organic

674         compounds in a boreal forest canopy and their relation to environmental and

675         biological factors, Atmospheric Chemistry and Physics, 9, 5447-5459, 2009.

676 Lewandowski, M., Jaoui, M., Offenberg, J. H., Kleindienst, T. E., Edney, E. O.,

677         Sheesley, R. J., and Schauer, J. J.: Primary and secondary contributions to

678         ambient PM in the midwestern United States, Environmental Science &

679         Technology, 42, 3303-3309, 2008.

680 Liu, Q. Y., Baumgartner, J., Zhang, Y., and Schauer, J. J.: Source apportionment of

681         Beijing air pollution during a severe winter haze event and associated

682         pro-inflammatory responses in lung epithelial cells, Atmospheric Environment,

683         126, 28-35, 10.1016/j.atmosenv.2015.11.031, 2016.

684 Lough, G. C., Christensen, C. G., Schauer, J. J., Tortorelli, J., Mani, E., Lawson, D. R.,

685         Clark, N. N., and Gabele, P. A.: Development of molecular marker source

686         profiles for emissions from on-road gasoline and diesel vehicle fleets, J. Air

687         Waste Manage. Assoc., 57, 1190-1199, 10.3155/1047-3289.57.10.1190, 2007.

688 Hallquist, M., Munthe, J., Hu, M., Wang, T., Chan, C. K., Gao, J., Boman, J., Guo, S.,

689         Hallquist, Å. M., and Mellqvist, J.: Photochemical smog in China: scientific

690         challenges and implications for air-quality policies, National Science Review, 3,

691         401-403, 2016.

Miyazaki, Y., Jung, J., Fu, P., Mizoguchi, Y., Yamanoi, K., and Kawamura, K.: Evidence of formation of submicrometer water‐soluble organic aerosols at a deciduous forest site in northern Japan in summer, Journal of Geophysical Research: Atmospheres, 117, 2012.

Offenberg, J. H., Lewis, C. W., Lewandowski, M., Jaoui, M., Kleindienst, T. E., and Edney, E. O.: Contributions of toluene and alpha-pinene to SOA formed in an irradiated toluene/alpha-pinene/NO(x)/ air mixture: comparison of results using 14C content and SOA organic tracer methods, Environmental Science & Technology, 41, 3972-3976, 2007.

Offenberg, J. H., Lewandowski, M., Edney, E. O., Kleindienst, T. E., and Jaoui, M.: Influence of Aerosol Acidity on the Formation of Secondary Organic Aerosol from Biogenic Precursor Hydrocarbons, Environ. Sci. Technol., 43, 7742-7747, 10.1021/es901538e, 2009.

Oros, D. R., and Simoneit, B. R. T.: Identification and emission rates of molecular tracers in coal smoke particulate matter, Fuel, 79, 515-536, Doi 10.1016/S0016-2361(99)00153-2, 2000.

Park, S. S., and Cho, S. Y.: Tracking sources and behaviors of water-soluble organic carbon in fine particulate matter measured at an urban site in Korea, Atmospheric environment, 45, 60-72, 2011.

Rogge, W. F., Hildemann, L. M., Mazurek, M. A., Cass, G. R., and Simoneit, B. R. T.: Sources of fine organic aerosol. 4. Particulate abrasion products from leaf surfaces of urban plants, Environ. Sci. Technol., 27, 2700-2711, 1993.

Saathoff, H., Naumann, K.-H., Möhler, O., Jonsson, Å. M., Hallquist, M., Kiendler-Scharr, A., Mentel, T. F., Tillmann, R., and Schurath, U.: Temperature dependence of yields of secondary organic aerosols from the ozonolysis of α-pinene and limonene, Atmos Chem Phys, 9, 1551-1577, 2009.

Schauer, J. J., Rogge, W. F., Hildemann, L. M., Mazurek, M. A., Cass, G. R., and Simoneit, B. R. T.: Source apportionment of airborne particulate matter using

720  organic compounds as tracers, Atmospheric Environment, 30, 3837-3855,

721  10.1016/1352-2310(96)00085-4, 1996.

722 Sheesley, R. J., Schauer, J. J., Zheng, M., and Wang, B.: Sensitivity of molecular

723  marker-based CMB models to biomass burning source profiles, Atmospheric

724  Environment, 41, 9050-9063, 2007.

725 Simoneit, B. R., Schauer, J. J., Nolte, C., Oros, D. R., Elias, V. O., Fraser, M., Rogge,

726  W., and Cass, G. R.: Levoglucosan, a tracer for cellulose in biomass burning and

727  atmospheric particles, Atmospheric Environment, 33, 173-182, 1999.

728 Song, G., Min, H., Qingfeng, G., and Dongjie, S.: Comparison of secondary organic

729  aerosol estimation methods, ACTA CHIMICA SINICA, 72, 658-666, 2014.

730 Song, Y., Zhang, Y., Xie, S., Zeng, L., Zheng, M., Salmon, L. G., Shao, M., and

731  Slanina, S.: Source apportionment of PM2. 5 in Beijing by positive matrix

732  factorization, Atmospheric Environment, 40, 1526-1537, 2006.

733 Stone, E. A., Nguyen, T. T., Pradhan, B. B., and Dangol, P. M.: Assessment of

734  biogenic secondary organic aerosol in the Himalayas, Environmental Chemistry,

735  9, 263-272, 2012.

736 Sun, J., Zhang, Q., Canagaratna, M. R., Zhang, Y., Ng, N. L., Sun, Y., Jayne, J. T.,

737  Zhang, X., Zhang, X., and Worsnop, D. R.: Highly time- and size-resolved

738  characterization of submicron aerosol particles in Beijing using an Aerodyne

739  Aerosol Mass Spectrometer, Atmospheric Environment, 44, 131-140, 2010.

740 Surratt, J. D., Kroll, J. H., Kleindienst, T. E., Edney, E. O., Claeys, M., Sorooshian, A.,

741  Ng, N. L., Offenberg, J. H., Lewandowski, M., Jaoui, M., Flagan, R. C., and

742  Seinfeld, J. H.: Evidence for organosulfates in secondary organic aerosol,

743  Environ. Sci. Technol., 41, 517-527, 10.1021/es062081q, 2007.

744 Surratt, J. D., Chan, A. W., Eddingsaas, N. C., Chan, M., Loza, C. L., Kwan, A. J.,

745  Hersey, S. P., Flagan, R. C., Wennberg, P. O., and Seinfeld, J. H.: Reactive

746  intermediates revealed in secondary organic aerosol formation from isoprene,

747  Proceedings of the National Academy of Sciences, 107, 6640-6645, 2010.

748  Tai, A. P., Mickley, L. J., and Jacob, D. J.: Correlations between fine particulate matter
749      (PM 2.5) and meteorological variables in the United States: Implications for the
750      sensitivity of PM 2.5 to climate change, Atmospheric Environment, 44,
751      3976-3984, 2010.

752  Tan, J. H., Duan, J. C., Chai, F. H., He, K. B., and Hao, J. M.: Source apportionment
753      of size segregated fine/ultrafine particle by PMF in Beijing, Atmospheric
754      Research, 139, 90-100, 10.1016/j.atmosres.2014.01.007, 2014.

755  Tao, J., Zhang, L., Cao, J., Zhong, L., Chen, D., Yang, Y., Chen, D., Chen, L., Zhang,
756      Z., Wu, Y., Xia, Y., Ye, S., and Zhang, R.: Source apportionment of PM2.5 at
757      urban and suburban areas of the Pearl River Delta region, south China - With
758      emphasis on ship emissions, Science of the Total Environment, 574, 1559-1570,
759      10.1016/j.scitotenv.2016.08.175, 2017.

760  Tian, S. L., Pan, Y. P., and Wang, Y. S.: Size-resolved source apportionment of
761      particulate matter in urban Beijing during haze and non-haze episodes, Atmos
762      Chem Phys, 16, 1-19, 10.5194/acp-16-1-2016, 2016.

763  Turpin, B. J., and Huntzicker, J. J.: Identification of secondary organic aerosol
764      episodes and quantitation of primary and secondary organic aerosol
765      concentrations during SCAQS, Atmospheric Environment, 29, 3527-3544, 1995.

766  Wang, B., Shao, M., Lu, S., Yuan, B., Zhao, Y., Wang, M., Zhang, S., and Wu, D.:
767      Variation of ambient non-methane hydrocarbons in Beijing city in summer 2008,
768      Atmospheric Chemistry and Physics, 10, 5911, 2010.

769  Wang, Q., Shao, M., Zhang, Y., Wei, Y., Hu, M., and Guo, S.: Source apportionment
770      of fine organic aerosols in Beijing, Atmospheric Chemistry and Physics, 9,
771      8573-8585, 2009.

772  Wang, X., Bi, X., Sheng, G., and Fu, J.: Chemical composition and sources of PM10
773      and PM2. 5 aerosols in Guangzhou, China, Environmental Monitoring and
774      Assessment, 119, 425-439, 2006.

775  Wong, J. P. S., Lee, A. K. Y., and Abbatt, J. P. D.: Impacts of Sulfate Seed Acidity and

776      Water Content on Isoprene Secondary Organic Aerosol Formation, Environ. Sci.

777      Technol., 49, 13215-13221, 10.1021/acs.est.5b02686, 2015.

778  Wu, Y., Guo, J., Zhang, X., and Li, X.: Correlation between PM concentrations and

779      Aerosol Optical Depth in eastern China based on BP neural networks,

780      Geoscience and Remote Sensing Symposium, 2011, 5876-5886.

781  Xiang, P., Zhou, X. M., Duan, J. C., Tan, J. H., He, K. B., Yuan, C., Ma, Y. L., and

782      Zhang, Y. X.: Chemical characteristics of water-soluble organic compounds

783      (WSOC) in PM2.5 in Beijing, China: 2011-2012, Atmos. Res., 183, 104-112,

784      10.1016/j.atmosres.2016.08.020, 2017.

785  Yang, F., Kawamura, K., Chen, J., Ho, K. F., Lee, S. C., Gao, Y., Cui, L., Wang, T. G.,

786      and Fu, P. Q.: Anthropogenic and biogenic organic compounds in summertime

787      fine aerosols (PM2.5) in Beijing, China, Atmospheric Environment, 124,

788      166-175, 10.1016/j.atmosenv.2015.08.095, 2016.

789  Yttri, K. E., Simpson, D., Nojgaard, J. K., Kristensen, K., Genberg, J., Stenstrom, K.,

790      Swietlicki, E., Hillamo, R., Aurela, M., Bauer, H., Offenberg, J. H., Jaoui, M.,

791      Dye, C., Eckhardt, S., Burkhart, J. F., Stohl, A., and Glasius, M.: Source

792      apportionment of the summer time carbonaceous aerosol at Nordic rural

793      background sites, Atmos Chem Phys, 11, 13339-13357, 2011.

794  Yu, L. D., Wang, G. F., Zhang, R. J., Zhang, L. M., Song, Y., Wu, B. B., Li, X. F., An,

795      K., and Chu, J. H.: Characterization and Source Apportionment of PM2.5 in an

796      Urban Environment in Beijing, Aerosol Air Qual Res, 13, 574-583,

797      10.4209/aaqr.2012.07.0192, 2013.

798  Zhang, H., Zhang, Z., Cui, T., Lin, Y.-H., Bhathela, N. A., Ortega, J., Worton, D. R.,

799      Goldstein, A. H., Guenther, A., Jimenez, J. L., Gold, A., and Surratt, J. D.:

800      Secondary Organic Aerosol Formation via 2-Methyl-3-buten-2-ol Photooxidation:

801      Evidence of Acid-Catalyzed Reactive Uptake of Epoxides, Environmental

802      Science & Technology Letters, 1, 242-247, 10.1021/ez500055f, 2014.

803    Zhang, Q., Streets, D. G., Carmichael, G. R., He, K. B., Huo, H., Kannari, A.,

804         Klimont, Z., Park, I. S., Reddy, S., Fu, J. S., Chen, D., Duan, L., Lei, Y., Wang, L.

805         T., and Yao, Z. L.: Asian emissions in 2006 for the NASA INTEX-B mission,

806         Atmos Chem Phys, 9, 5131-5153, 2009.

807    Zhang, R., Jing, J., Tao, J., Hsu, S.-C., Wang, G., Cao, J., Lee, C. S. L., Zhu, L., Chen,

808         Z., and Zhao, Y.: Chemical characterization and source apportionment of PM 2.5

809         in Beijing: seasonal perspective, Atmos Chem Phys, 13, 7053-7074, 2013.

810    Zhang, Y. X., Sheesley, R. J., Schauer, J. J., Lewandowski, M., Jaoui, M., Offenberg, J.

811         H., Kleindienst, T. E., and Edney, E. O.: Source apportionment of primary and

812         secondary organic aerosols using positive matrix factorization (PMF) of

813         molecular markers, Atmospheric Environment, 43, 5567-5574, 2009.

814    Zhang, Y., Cai, J., Wang, S., He, K., and Zheng, M.: Review of receptor-based source

815         apportionment research of fine particulate matter and its challenges in China,

816         The Science of the total environment, 586, 917-929,

817         10.1016/j.scitotenv.2017.02.071, 2017.

818    Zheng, J., Hu, M., Peng, J., Wu, Z., Kumar, P., Li, M., Wang, Y., and Guo, S.: Spatial

819         distributions and chemical properties of PM 2.5 based on 21 field campaigns at

820         17 sites in China, Chemosphere, 159, 480-487, 2016a.

821    Zheng, M., Salmon, L. G., Schauer, J. J., Zeng, L., Kiang, C., Zhang, Y., and Cass, G.

822         R.: Seasonal trends in PM2. 5 source contributions in Beijing, China,

823         Atmospheric Environment, 39, 3967-3976, 2005.

824    Zheng, X. X., Guo, X. Y., Zhao, W. J., Shu, T. T., Xin, Y. A., Yan, X., Xiong, Q. L.,

825         Chen, F. T., and Lv, M.: Spatial variation and provenance of atmospheric trace

826         elemental deposition in Beijing, Atmos. Pollut. Res., 7, 260-267,

827         10.1016/j.apr.2015.10.006, 2016b.

828    Zhou, J. B., Xiong, Y., Xing, Z. Y., Deng, J. J., and Du, K.: Characterizing and

829         sourcing ambient PM2.5 over key emission regions in China II: Organic

830      molecular markers and CMB modeling, Atmospheric Environment, 163, 57-64,

831      10.1016/j.atmosenv.2017.05.033, 2017.

832   Zhu, C., Kawamura, K., and Fu, P.: Seasonal variations of biogenic secondary organic

833      aerosol tracers in Cape Hedo, Okinawa, Atmospheric Environment, 130, 113-119,

834      10.1016/j.atmosenv.2015.08.069, 2016.

835   Zhu, Y., Yang, L., Kawamura, K., Chen, J., Ono, K., Wang, X., Xue, L., and Wang, W.:

836      Contributions and source identification of biogenic and anthropogenic

837      hydrocarbons to secondary organic aerosols at Mt. Tai in 2014, Environmental

838      Pollution, 220, 863-872, 10.1016/j.envpol.2016.10.070, 2017.

**Table**

Table 1. Summer $PM_{2.5}$ mass concentrations in Beijing from 2008-2016, average $\pm$ standard deviation ($\mu g\ m^{-3}$).

| Year/Month | 2008/07 | 2009/07 | 2010/05 | 2016/05-06 | 2016/05-06 |
|---|---|---|---|---|---|
| Site | PKUERS | PKUERS | PKUERS | CP | PKUERS |
| | ($\mu g\ m^{-3}$) | ($\mu g\ m^{-3}$) | ($\mu g\ m^{-3}$) | ($\mu g\ m^{-3}$) | ($\mu g\ m^{-3}$) |
| $PM_{2.5}$ | 92.3±44.7 | 88.2±52.3 | 62.7±36.5 | 43.0±17.5 | 45.5±19.8 |
| OC | 10.4±2.9 | 8.5±2.5 | 8.9±4.5 | 8.9±3.2 | 11.0±3.7 |
| EC | 3.3±1.5 | 2.5±0.9 | 2.1±1.1 | 0.7±0.5 | 1.8±1.0 |
| $SO_4^{2-}$ | 35.6±24.7 | 25.5±18.6 | 11.8±9.8 | 7.9±5.7 | 4.7±3.4 |
| $NO_3^-$ | 7.9±6.9 | 17.8±13.2 | 10.0±11.2 | 3.4±3.3 | 2.4±2.3 |
| $NH_4^+$ | 15.2±11.3 | 13.5±8.4 | 5.9±5.9 | 4.6±3.0 | 3.5±3.5 |
| Ref. | (Guo et al., 2012) | (Zheng et al., 2016a) | (Zheng et al., 2016a) | This study | This study |

**Figure captions**

Fig. 1 Concentrations of organic carbon from primary and secondary organic sources at (a) CP and (b) PKUERS as well as their contributions to the measured organic carbon at (c) CP and (d) PKUERS (%).

Fig. 2 Comparison of the sources at PKUERS between 2016 and 2008

Fig. 3 Particle sources from different air mass origins

Fig. 4 Correlations between SOC and different influencing factors (a)-(b) ozone, (c)-(d) temperature, (e)-(f) water and (g)-(h) $H^+$ concentratio
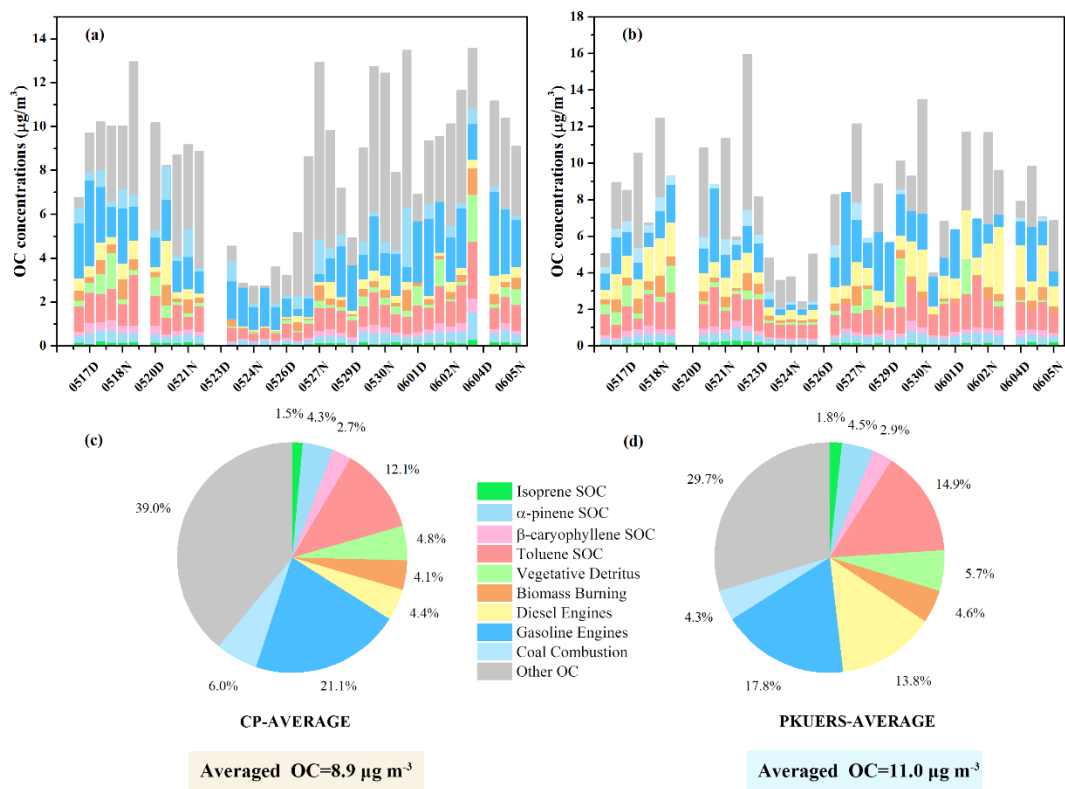
Fig. 1 Concentrations of organic carbon from primary and secondary organic sources at (a) CP and (b) PKUERS as well as their contributions to the measured organic carbon at (c) CP and (d) PKUERS (%).
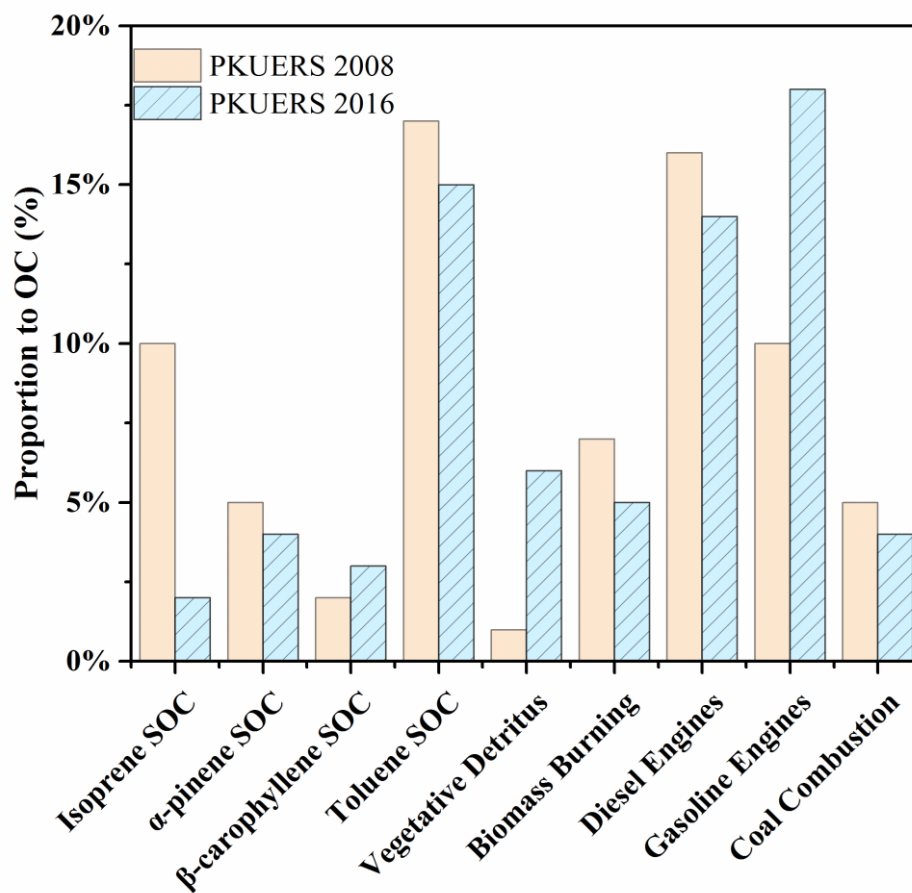
Fig.2 Comparison of the sources at PKUERS between 2016 and 2008 (Guo et al. 2012)
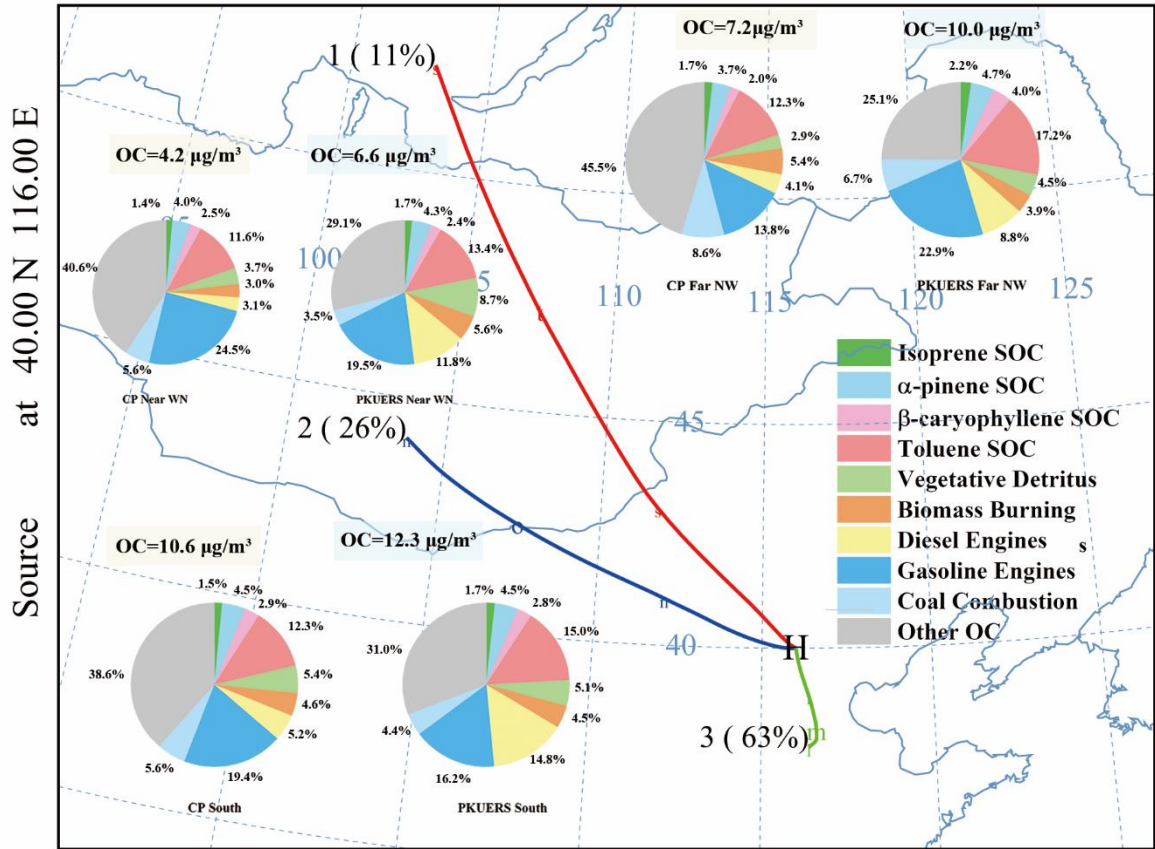
Fig. 3 Particle sources from different air mass origins
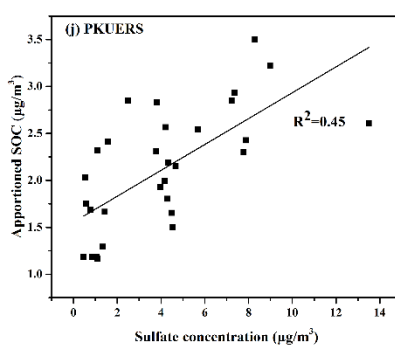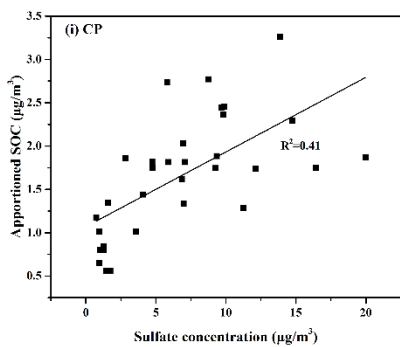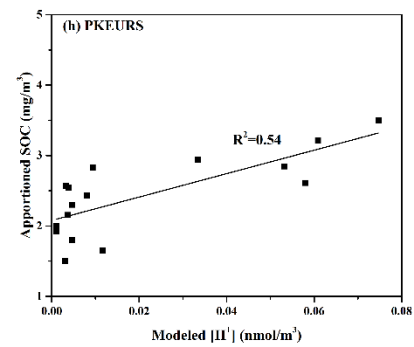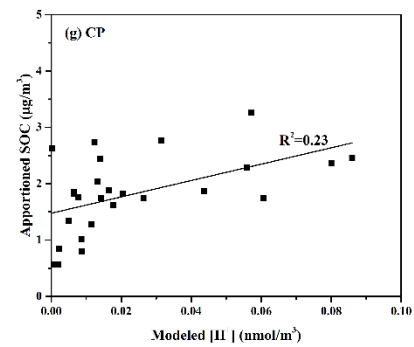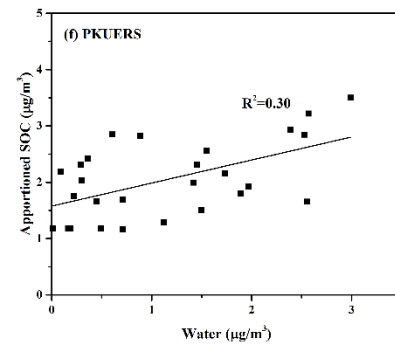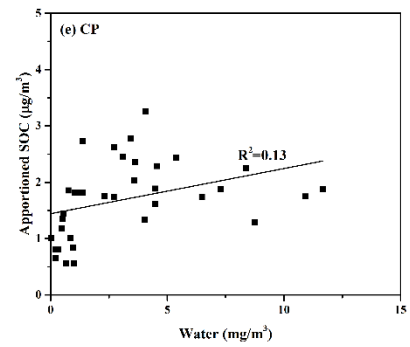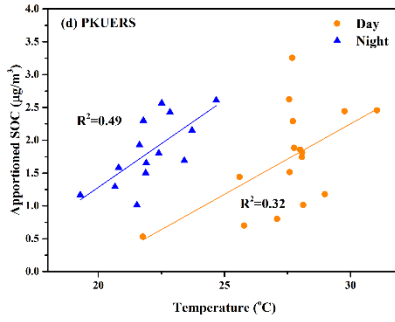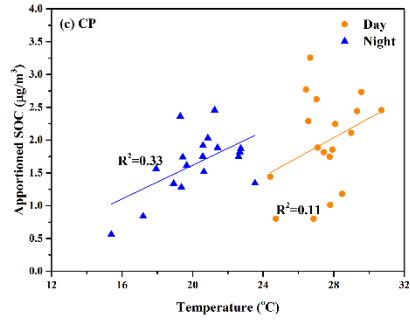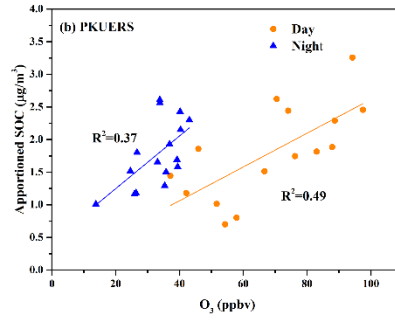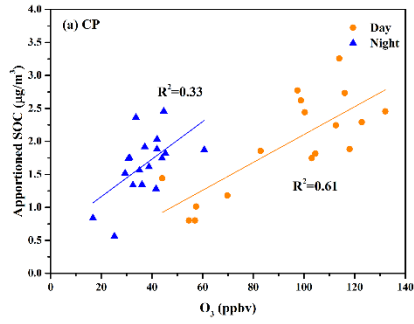
Fig. 4 Correlations between SOC and different influencing factors (a)-(b) ozone, (c)-(d) temperature, (e)-(f) water and (g)-(h) H$^+$ concentration (i)-(j) sulfate concentration